34th Annual International Conference of the IEEE EMBS
San Diego, California USA, 28 August - 1 September, 2012

4D human body posture estimation based on a motion capture system and a multi-rigid link model

Naoya Yoshikawa, Yasuyuki Suzuki, Wataru Ozaki, Tomohisa Yamamoto, and Taishin Nomura

Abstract— **Human motion analysis in various fields such as neurophysiology, clinical medicine, and sports sciences utilizes a multi-rigid link model of a human body for considering kinetics by solving inverse dynamics of a motion, in which a motion capture system with reflective markers are often used to measure the motion, and then the obtained motion are mapped onto the multi-rigid link model. However, algorithms for such a mapping from spatio-temporal positions of the markers to the corresponding posture of the model are not always fully disclosed. Moreover, a common difficulty for such algorithms is an error caused by displacements of the markers attached on the body surface, referred to as the skin motion error. In this study, we developed a simple algorithm that maps positions of the markers to the corresponding posture of a rigid link model, and examined accuracy of the algorithm by evaluating quantitatively differences between the measured and the estimated posture. We also analyzed the skin motion error. It is shown that magnitude of the error was determined not only by the amplitude of the skin motion, but also by the direction of the marker displacement relative to the frame of reference attached to each segment of the body.**

I. Introduction

HUMAN motions are realized through interactions among neural, muscular, and skeletal systems, as well as environment. Human motion analysis has been utilized in various fields such as neurophysiology, orthopedic and neurological medicine, and sports sciences. For a better understanding of dynamic mechanisms during human movement, kinematic measurements using a motion capture system and analyses using a multi-rigid link model of the human body consisted of multiple rigid links and joints are often performed [1]. Joint torques during human motion can then be calculated by the inverse dynamics method using equations of motion of the multi-rigid link model that moves according to the measured human motion. The obtained joint torques provide important information to explore underlying motor control mechanisms during human motion [2].

It is necessary for representing a human motion using a multi-rigid link model to estimate dynamic changes in positions and postures of every body segment based on a kinematic motion data obtained usually from a motion capture system that provides spatio-temporal positions of reflective markers attached on the body surface. Note that the human body segments are not rigid and they are not necessarily connected by simple joint mechanisms. A number of software is available for this purpose with algorithms for a mapping from spatio-temporal position of the markers to the corresponding posture of the rigid link model. However, they are not always fully disclosed. Moreover, a common challenge for such algorithms is to reduce an effect of marker displacement on the body surface, referred to as the skin motion error [3], [4], which lowers the accuracy of posture estimation and can cause unexpected errors in the inverse dynamics analysis.

Here we developed a simple algorithm for the mapping from positions of the markers on the body surface to the corresponding posture of a rigid link model. For validating the algorithm, we evaluated differences (errors) between the measured and the estimated posture along a motion. We then analyzed the skin motion errors. It was shown that the magnitude of error was determined not only by the amplitude of the skin motion, but also by the direction of the marker displacement relative to the frame of reference attached to each segment of the body.

II. Posture Estimation Algorithm

Let us consider a rigid link model as a body segment in a space. We represent a motion of the rigid link using a position (translation) and a posture (angular rotation) specified with respect to the global coordinate fixed in the space. To this end, we define an orthogonal coordinate system that translates and rotates together with the rigid link, referred to as the local coordinate (Fig. 1(a)). The position of the rigid link is represented by a three dimensional vector from the origin of the global coordinate to the origin of the local coordinate, denoted as $\mathbf{o}$. The posture of the link is represented by an angular rotation between the global and the local coordinates. The posture of the rigid link (the local coordinate) is described by the matrix $\mathbf{A}=[\mathbf{e}_x\ \mathbf{e}_y\ \mathbf{e}_z]$, where $\mathbf{e}_x$, $\mathbf{e}_y$, and $\mathbf{e}_z$ are the unit basis vectors of the local coordinate represented by the global coordinate. We use x-y-z Euler angles $(\varphi, \theta, \psi)^T$ to represent the posture, which is calculated from the matrix $\mathbf{A}$.

We model the human body using multi-rigid links connected by spherical joints in the space, assuming a hierarchical tree structure from a top link to lower links. A position and a posture of a lower link (child link) are represented by a relative position and relative posture from the immediate upper link (parent link) in the local coordinate

Manuscript received March 29, 2012. This work was supported in part by JSPS grants-in-aid 21-416 and 23300166, MEXT Global COE Program "in silico medicine" at Osaka University.

N. Yoshikawa, Y. Suzuki, W. Ozaki, T. Yamamoto, and T. Nomura are with Graduate School of Engineering Science at Osaka University, Toyonaka, Osaka, 560-8531 Japan (phone: +81-6-6850-6534; fax: +81-6-6850-6534; e-mail: yoshikawa@bpe.es.osaka-u.ac.jp, suzuki@bpe.es.osaka-u.ac.jp, ozaki@bpe.es.osaka-u.ac.jp, yamamoto@bpe.es.osaka-u.ac.jp, taishin@bpe.es.osaka-u.ac.jp).

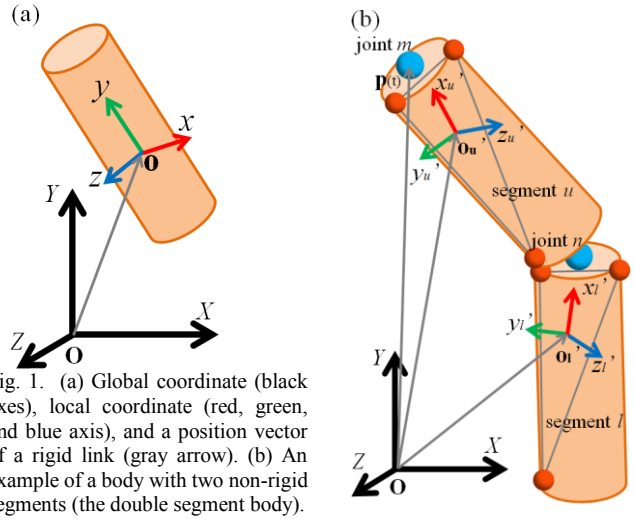

Fig. 1. (a) Global coordinate (black axes), local coordinate (red, green, and blue axis), and a position vector of a rigid link (gray arrow). (b) An example of a body with two non-rigid segments (the double segment body).

of parent link. The relative posture of a child link is described as $\mathbf{A_p}^{-1}\mathbf{A_c}$, where $\mathbf{A_p}$ and $\mathbf{A_c}$ are the postures of the parent and the child link, respectively, in the global coordinate.

A human body can be considered as a hierarchical combination of multiple body segments that are distinguished from the links of the human body model because they are not really rigid. We define the mapping that associates a position and a posture of each body segment with those of the corresponding rigid link. To this end, we specify the position and the posture of each body segment from markers attached on the surface of the segment by defining a local coordinate also for the segment. A position and a posture of a segment at a time instant are estimated from positions of characteristic points defined anatomically for each body segment of the human body in [5]. The reflective markers were attached on the surface of each body segment so that they could specify the characteristic points.

Let us illustrate how we define the local coordinate for a given segment using an example of a body-like object with two segments (the double segment body with the segment-*u* and the segment-*l*) with several attached markers (Fig. 1(b) where positions of the attached markers are arbitrary in this simple example, but they should be at specific locations for the human body). Note that the segments are not rigid but deformable. Suppose the position of the proximal joint (joint *m*) of the segment-*u* can be obtained in the global coordinate as $\mathbf{p}(t)$ to which the segment-*u* is connected by a spherical joint, and the proximal end of the segment-*l* is connected with the distal end of the segment-*u* by a spherical joint (joint *n*).

Step-1: We define a tentative local coordinate for the segment-*u* with the axes $\boldsymbol{x_u}$', $\boldsymbol{y_u}$', and $\boldsymbol{z_u}$' that moves together with the segment-*u* using position of three markers attached on the segment-*u*. The origin $\mathbf{o_u}'(t)$ of the tentative local coordinate at time *t* is defined as the gravity center of the triangle formed by the markers at time *t* as vertices in the global coordinate. $\boldsymbol{x_u}'(t)$ axis at time *t* is defined as a unit vector directing from the $\mathbf{o_u}'(t)$ to the incenter of the triangle. $\boldsymbol{z_u}'(t)$ axis at time *t* is defined as a unit vector perpendicular to the plane formed by the triangle. $\boldsymbol{y_u}'(t)$ axis at time *t* is defined as a unit vector perpendicular to both $\boldsymbol{x_u}'(t)$ and $\boldsymbol{z_u}'(t)$ axes. Posture of the tentative local coordinate $\mathbf{A_u}'(t)$ of the segment-*u* at time *t* is then defined as the matrix $[\boldsymbol{x_u}'(t)\ \boldsymbol{y_u}'(t)\ \boldsymbol{z_u}'(t)]$. Position and posture of the tentative local coordinate of the segment-*l* is defined similarly, and represented by the $\mathbf{o_l}'(t)$ and $\mathbf{A_l}'(t)=[\boldsymbol{x_l}'(t)\ \boldsymbol{y_l}'(t)\ \boldsymbol{z_l}'(t)]$, respectively. Note that the position of each marker relative to each segment may slide due to deformation of the segment and the skin motion, meaning that the positions of $\mathbf{o_u}'$ and $\mathbf{o_l}'$ relative to the corresponding segments and the matrices $\mathbf{A_u}'$ and $\mathbf{A_l}'$, which should be constant throughout the motion if the segments are rigid, change temporally.

Step-2: Using $\mathbf{o_u}'(t)$, $\mathbf{A_u}'(t)$, $\mathbf{o_l}'(t)$, and $\mathbf{A_l}'(t)$ for the segments, the positions of the joints *m* and *n* at time *t*, referred to as $\mathbf{j_m}(t)$ and $\mathbf{j_n}(t)$, are described as follows;

$$\mathbf{j_m}(t) = \mathbf{o_u}'(t) + \mathbf{A_u}'(t)\ \mathbf{r_{um}}(t) \tag{1}$$

$$\mathbf{j_n}(t) = \mathbf{o_u}'(t) + \mathbf{A_u}'(t)\ \mathbf{r_{un}}(t) = \mathbf{o_l}'(t) + \mathbf{A_l}'(t)\ \mathbf{r_{ln}}(t) \tag{2}$$

where $\mathbf{r_{um}}(t)$ and $\mathbf{r_{un}}(t)$ are the vectors pointing the joint *m* and joint *n* from the $\mathbf{o_u}'(t)$ in the tentative local coordinate of the segment-*u*, respectively. $\mathbf{r_{ln}}(t)$ is the vector pointing the joint *n* from the $\mathbf{o_l}'(t)$ in the tentative local coordinate of the segment-*l*. If the segments are rigid, three vectors ($\mathbf{r_{um}}(t)$, $\mathbf{r_{un}}(t)$, $\mathbf{r_{ln}}(t)$) should also be constant throughout the motion. However, they change over time due to the skin motion. Nevertheless, we need to determine those three vectors as the approximated constant values so that each tentative local coordinate can be mapped to the local coordinate of the corresponding rigid link. To this end, the approximated constant values $\bar{\mathbf{r}}_{\mathbf{um}}$, $\bar{\mathbf{r}}_{\mathbf{un}}$, and $\bar{\mathbf{r}}_{\mathbf{ln}}$ were obtained so that they minimize the square sum of differences between the terms in the middle and the most right-hand-side of Eq. (2) over the motion time,

$$\sum_t \left|(\mathbf{o_u}'(t) + \mathbf{A_u}'(t)\ \bar{\mathbf{r}}_{\mathbf{un}}) - (\mathbf{o_l}'(t) + \mathbf{A_l}'(t)\ \bar{\mathbf{r}}_{\mathbf{ln}})\right|^2 \tag{3}$$

which forces two segments to be connected at the identical point (the joint *n*) as much as possible. The obtained vectors can estimate the length of the segment-*u* as $|\bar{\mathbf{r}}_{\mathbf{um}} - \bar{\mathbf{r}}_{\mathbf{un}}|$.

Consequently, we obtain a set of modified tentative local coordinates for the segments that can be used consistently for representing the corresponding motion of the double rigid link model of the double segment body. That is, the postures $\mathbf{A_u}'(t)$ and $\mathbf{A_l}'(t)$ of the modified tentative local coordinates remain unchanged, but the modified positions $\mathbf{O_u}'(t)$ of the segment-*u* and $\mathbf{O_l}'(t)$ of the segment-*l* at time *t* are defined as follows;

$$\mathbf{O_u}'(t) = \mathbf{p}(t) - \mathbf{A_u}'(t)\ \bar{\mathbf{r}}_{\mathbf{um}} \tag{4}$$

$$\mathbf{O_l}'(t) = \mathbf{O_u}'(t) + \mathbf{A_u}'(t)\ \bar{\mathbf{r}}_{\mathbf{um}} - \mathbf{A_l}'(t)\ \bar{\mathbf{r}}_{\mathbf{ln}} \tag{5}$$

by forcing $\mathbf{j_m}(t)$ to be identical with $\mathbf{p}(t)$. Note that, for the modified tentative coordinates, the equality

$$(\mathbf{O_u}'(t) + \mathbf{A_u}'(t)\ \bar{\mathbf{r}}_{\mathbf{um}}) - (\mathbf{O_l}'(t) + \mathbf{A_l}'(t)\ \bar{\mathbf{r}}_{\mathbf{ln}}) = \mathbf{0} \tag{6}$$

always holds, and the distance between two joints is constant. By identifying the modified tentative local coordinate of each segment $\{\mathbf{O_u}'(t),\ \mathbf{A_u}'(t),\ \mathbf{O_l}'(t),\ \mathbf{A_l}'(t)\}$ with the local coordinate of the corresponding rigid link $\{\mathbf{o_u}(t),\ \mathbf{A_u}(t),\ \mathbf{o_l}(t),$

$\mathbf{A_l}(t)\}$, the mapping from the positions of the markers on the body surface to the corresponding posture of the rigid link model for this example is defined as;

$$\text{Positions of the markers} \rightarrow \{\mathbf{o_u}(t), \mathbf{A_u}(t), \mathbf{o_l}(t), \mathbf{A_l}(t)\} \quad (7)$$

where $\mathbf{o_u}(t)=\mathbf{O_u'}(t)$, $\mathbf{A_u}(t)=\mathbf{A_u'}(t)$, $\mathbf{o_l}(t)=\mathbf{O_l'}(t)$, $\mathbf{A_l}(t)=\mathbf{A_l'}(t)$.

Step-3: This step is optional, but useful for standardization in describing human motions. The local coordinate system of each segment is re-defined based on the modified tentative coordinate obtained in Step-2. For the human body, the standardized local coordinate of each body segment is proposed by [5], specifying the location and posture of each human body segment. In this study, the modified tentative local coordinate for each body segment is transformed so that it becomes identical with the one by [5].

III. Validation Method of Algorithm Accuracy and Effect Analysis of Skin Motion Error

For validating our algorithm, a motion during human gait on a treadmill was captured. We used an optoelectronic motion analysis system (SMART-DX, BTC, Italy) for capturing the gait motion. In particular, we measured the motion of the right lower leg by assuming four segments for the right leg. The top segment corresponds to the pelvis, and the remaining three segments to the thigh, the shank, and the foot (Fig. 2). Three or four infrared reflection markers of diameters 1.0 cm were put on each segment (TABLE I). Marker positions are captured with 8 infrared cameras with the sampling frequency 300 Hz. In this sequel, a position of the i-th marker at time t is denoted as $(x_i(t), y_i(t), z_i(t))$ in the global coordinate. Positions of reflective markers attached to the characteristic points defined by [5] and the local coordinate system for each segment obtained as in Eq. (7) with Step-3 are shown in Fig. 2. As in II, we assume that any two adjacent segments are connected by a spherical joint. Then the measured positions of the markers were mapped on the four-rigid link model corresponding to the four-segment leg. The obtained motion of the rigid link model was visualized using an integrated development environment for physiological modeling called *insilico*IDE [6].

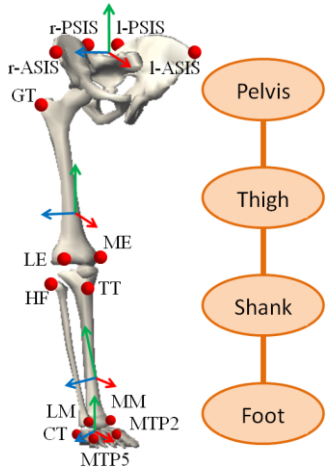

Fig. 2. Positions of reflective markers and local coordinate systems

TABLE I. Positions of a marker.

r-ASIS	right-anterior superior iliac spine
l-ASIS	left-anterior superior iliac spine
r-PSIS	right-posterior superior iliac spine
l-PSIS	left-posterior superior iliac spine
GT	greater trochanter
LE	lateral epicondyle
ME	medial epicondyle
TT	tibial tuberosity
HF	head of fibula
LM	lateral malleolus
MM	medial malleolus
CT	calcaneal tuberosity
MTP2	metatarsophalangeal joint of the second toe
MTP5	metatarsophalangeal joint of the little toe

A. Validation of posture estimation

For validating accuracy of the posture estimation, we consider "virtual markers (v-markers)" that are fixed to the rigid links. Differences between positions of the real markers and those of the v-markers represent the errors in the posture estimation with the multi rigid link model. Let us consider a real maker attached on a body segment. The position of the corresponding v-marker that is fixed to the corresponding link is defined as a mean position of the real marker over the measured motion in the local coordinate for the link. We denote the position of the i-th v-marker corresponding to the i-th real marker at time t as $(x_i'(t), y_i'(t), z_i'(t))$ in the global coordinate. The distance between the i-th real marker and the i-th v-marker,

$$\sqrt{(x_i(t) - x_i'(t))^2 + (y_i(t) - y_i'(t))^2 + (z_i(t) - z_i'(t))^2} \quad (8)$$

represents the error of our posture estimation at time t.

B. Effect of marker displacement on body surface

We analyze the effect of skin motion error [3], [4] which is known as the displacement of markers on the body surface due to several reasons such as volume change of muscles and tendon expansion. Here we consider effect of the skin motion in the thigh segment on the posture estimation. Positions of three markers on the thigh are shown in Fig. 2. We define the matrix $\tilde{\mathbf{A}}$ to represent the thigh posture if the markers are exactly on those characteristic points without displacement and the corresponding Euler angle $(\tilde{\varphi}, \tilde{\theta}, \tilde{\psi})^T$. We also consider the matrix $\mathbf{A'}$ for the thigh posture assuming one of three markers is displaced in the direction of either x, y, or z axis of the local coordinate for the thigh and the corresponding Euler angle $(\varphi', \theta', \psi')^T$. We assumed time-dependent sinusoidal displacement with amplitude of 1 cm. Note that the rotations around x, y, and z axes of the local coordinate correspond to adduction/abduction, inner/external rotation, and bending /stretching of the thigh, respectively, for the local coordinate defined in Step-3 of II. We calculated the $(\varphi_e, \theta_e, \psi_e)^T$ angular difference between $(\tilde{\varphi}, \tilde{\theta}, \tilde{\psi})^T$ and $(\varphi', \theta', \psi')^T$ to evaluate the error due to the skin motion.

IV. Results

Fig. 3(a) shows the gait motion and the estimated sequence of motion of the corresponding rigid-link model, displaying a good correspondence between them at least qualitatively.

A. Validation of posture estimation

Fig. 3(b) shows the trajectories of the measured markers and the corresponding v-markers during movement shown in Fig. 3(a). Black trajectories are for the measured makers attached at GT, TT, and MTP2 (see Fig. 2). Red, green, and blue trajectories are for the corresponding v-markers, referred to here as v-GT, v-TT, and v-MTP2. Fig. 3(c) shows the time courses of the errors defined as Eq. (8) for those sets of markers. The errors (average±variance) for GT and v-GT, TT and v-TT, and MTP2 and v-MTP2 were 0.609±0.233 cm, 0.770±0.244 cm, and 0.935±0.418 cm, respectively.

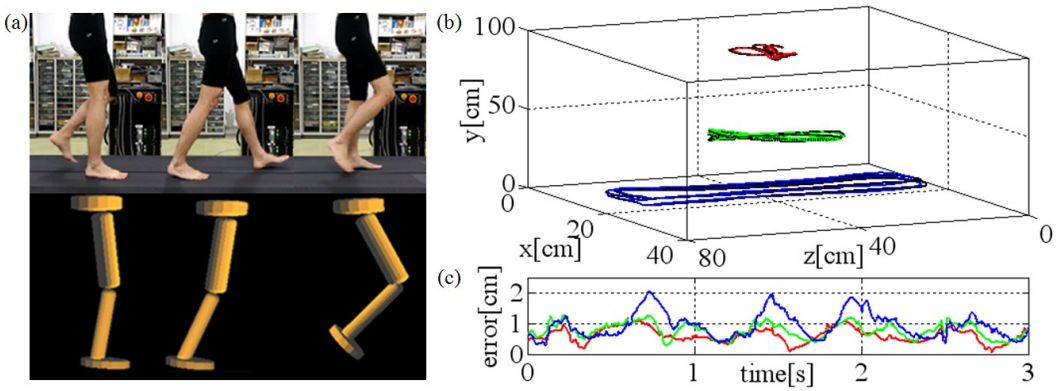

Fig. 3. (a) An example of reproduction result on computer during human gait movement with photographs of lower leg. (b) Trajectories of virtual and measured markers. Red, green, and blue trajectories are for v-GT, v-TT, and v-MTP2, respectively. Black trajectories are for the measured markers. (c) Errors between measured marker and virtual marker. Red, green, and blue lines are time-series data of GT, TT, and MTP2, respectively.

B. *Effect of marker displacement on body surface*

Fig. 4 shows the posture estimation errors for testing sinusoidal skin motions in three directions. Top, middle, and bottom rows of Fig. 4 show the posture estimation errors due to the displacement of GT, LE, and ME, respectively. Left, center, and right columns of Fig. 4 show the posture estimation error due to the displacement of markers in the directions of x, y, and z axes, respectively. The estimation error was the largest when the marker was displaced in the direction of the x axis among three displacement directions. In particular, when LE and ME were displaced 1 cm in the x direction, the estimation errors in θ were about 5.2 degree. When GT was displaced 1 cm in the x direction, φ and θ were estimated correctly, but ψ was estimated with the error of about 0.5 degree. On the other hand, the effect of marker displacement in the y and z directions was not as large as that in the x direction. The maximum error was caused by the displacement of ME in the y direction (0.5 degree in φ).

V. Conclusion and Discussion

We developed the posture estimation algorithm for the mapping from positions of the markers on the body surface to the corresponding posture of the multi-rigid link model. Accuracy of the algorithm was examined by comparing positions of the measured markers and the corresponding virtual markers of the rigid link model. The averaged error between the measured and the virtual markers at thigh, shank, and foot was about 0.77 cm. We also analyzed the effect of marker displacement on the posture estimation, and showed that the magnitude of error was determined by not only the amplitude but also direction of the displacement.

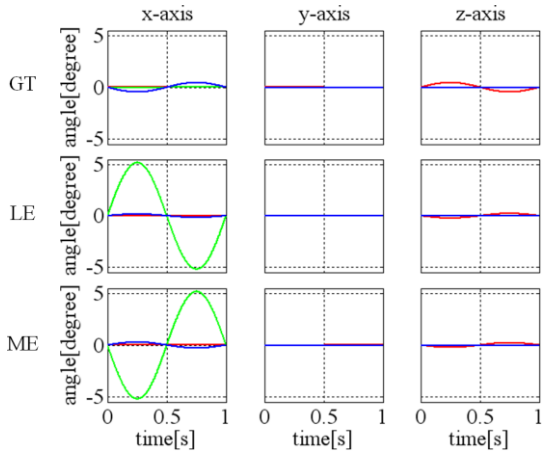

Fig. 4. Posture estimation error due to the displacement of marker. (red line: angle φ_e, green line: angle θ_e, blue line: angle ψ_e)

Let us discuss about how the marker displacement and the resulting posture estimation error affect the motion analysis with inverse dynamics. It is known that the maximum bending and stretching, adduction and abduction, and inner rotation and external rotation at hip joint during human gait are 45, 10, and 12 degree, respectively [7]. The maximum error in the posture estimation due to the marker displacement of the amplitude of 1.0 cm was 5.2 degree in θ, which was caused by the displacement in the x direction. The θ is rotation angle around the y axis, corresponding to the inner/external rotation. This suggests that the marker displacement on the body skin can produce a large error, comparable to the amount of hip joint motion during gait in the inner/external rotation. This means that the marker displacement on the body surface can largely influence on the motion analysis. In order to obtain joint torques accurately using inverse dynamics, it is required to develop new algorithms and to examine better positions of markers so that we can reduce the errors.

References

[1] Yong-You Ma, Hui Zhang, and Shou-Wei Jiang, "Realistic Modeling and Animation of Human Body Based on Scanned Data", *J Comput Sci Technol*, 19(4), 529-537, 2004

[2] M. Wojtyra, "Multibody Simulation Model of Human Walking", *Mech. Based Des. Struct. Mach.*, 31(3), 357-379, 2003.

[3] A. Cappozzo, F. Catani, A. Leardini, M. G. Benedetti, and U. D. Croce. "Position and orientation in space of bones during movement: experimental artefacts", *Clin Biomech*, 11(2). 90-100, 1996

[4] E. J. Alexander, T. P. Andriacchi, "Correcting for deformation in skin-based marker systems", *J Biomech*, 34(3), 355-361, 2001.

[5] U. D. Croce, A. Cappozzo, and D. C. Kerrigan, "Pelvis and lower limb anatomical landmark calibration precision and its propagation to bone geometry and joint angles", *Med Biol Eng Comput*, 37(2), 155-161, 1999

[6] Y. Suzuki, Y. Asai, T. Kawazu, M. Nakanizhi, Y. Taniguchi, E. Heien, K. Hagihara, Y. Kurachi, and T. Nomura, "A Platform for in silico Modeling of Physiological Systems II. CellML Compatibility and Other Extended Capabilities", *Proceedings of the 30th Annual International Conference of the IEEE EMBS*, EMBC 2008, Vancouver, BC Canada, no. 4649217, pp. 573-576

[7] C. W. Chan, A. Rudins, "Foot biomechanics during walking and running", *Mayo Clin. Proc.* 69(5), 448-461, 1994